

## REAL EVAPOTRANSPIRATION OF COCONUT - DWARF DETERMINED BY THE PARAMETRIZED METRIC MODEL IN SEMI-ARID PARAIBANO

MAILSON ARAÚJO CORDÃO <sup>2</sup>; RENATA RICHELLE SANTOS DINIZ <sup>3</sup>; HUGO ORLANDO CARVALLO GUERRA <sup>4</sup> AND CRIS LAINY MACIEL SANTOS <sup>5</sup>

<sup>1</sup> Work originating from the first author's Doctoral Thesis.

<sup>2</sup> Agricultural Engineer, PhD in Agricultural Engineering, Federal University of Campina Grande, Street: Aprígio Veloso, 882, Bairro Universitário, Bodocongó, CEP: 58429-900. Campina Grande, Paraíba, Brazil. [mailson.cordao@gmail.com](mailto:mailson.cordao@gmail.com).

<sup>3</sup> Biosystems Engineer, PhD student in Agricultural Engineering, Federal University of Campina Grande, Rua: Aprígio Veloso, 882, Bairro Universitário, Bodocongó, CEP: 58429-900. Campina Grande, Paraíba, Brazil. [renatarichelle1993@gmail.com](mailto:renatarichelle1993@gmail.com).

<sup>4</sup> Agricultural Engineer PhD Full Professor, Academic Unit of Agricultural Engineering, Federal University of Campina Grande, Street: Aprígio Veloso, 882, Bairro Universitário, Bodocongó, CEP: 58429-900, Campina Grande, Paraíba, Brazil, [hugoguerra1946@gmail.com](mailto:hugoguerra1946@gmail.com).

<sup>5</sup> Agricultural Engineer, PhD in Agricultural Engineering Federal University of Campina Grande, Rua: Aprígio Veloso, 882, Bairro Universitário, Bodocongó, CEP: 58429-900, Campina Grande, Paraíba, Brazil, [crislainymacielsantos@gmail.com](mailto:crislainymacielsantos@gmail.com).

### 1 RESUMO

A região do nordeste é a maior produtora de coco verde, motivada pelo uso da irrigação, a qual tem como critério de ser cada vez mais eficiente a longo dos anos. O objetivo desse trabalho foi estimar a evapotranspiração real diária pelo modelo METRIC (*Mapping evapotranspiration at high resolution with internalized calibration*) parametrizado utilizando dados espectrais de imagens de satélite do Landsat-8 e dados meteorológicos, e comparar as estimativas da Evapotranspiração real diária (ETa) com o método de Penman-Monteith, em uma área implantada com coqueiro-anão irrigado no município de Sousa, PB. A ETa foi estimada a partir da densidade do fluxo de calor latente, obtida como resíduo do balanço de energia pelo modelo METRIC parametrizado, que inclui em sua implementação, calibração radiométrica, cômputo da reflectância e de variáveis biofísicas, balanço de radiação, fluxo do calor no solo e processos iterativos parametrizados para obtenção do calor sensível. O saldo de radiação, fluxo do calor no solo e evapotranspiração real estimados pelo METRIC parametrizado permitiram a obtenção da influência da sazonalidade nas épocas do ano e da condição hídrica na cultura do coqueiro-anão irrigado. O METRIC parametrizado apresentou eficácia na estimativa da evapotranspiração real diária na cultura do coqueiro irrigado no período de estiagem.

**Palavras-chave:** *cocos nucifera*, demanda hídrica, sensoriamento remoto, semiárido brasileiro.

## CORDÃO, MA; DINIZ, RRS; WAR, HOC; SANTOS, CLM REAL EVAPOTRANSPIRATION OF DWARF COCONUT TREE DETERMINED BY THE PARAMETERIZED METRIC MODEL IN THE PARAIBAN SEMIARID

### 2 ABSTRACT

The northeast region is the largest producer of green coconut, motivated by the use of irrigation, which has the criterion of being increasingly efficient over the years. The objective of this work was to estimate the actual daily evapotranspiration by the parameterized METRIC model (mapping evapotranspiration at high resolution with internalized calibration) using spectral data from Landsat-8 satellite images and meteorological data and to compare the ET estimates with the Penman method - Monteith, in an area planted with irrigated dwarf coconut trees in the municipality of Sousa, PB. The ETa was estimated from the density of the latent heat flux, obtained as a residue of the energy balance by the parameterized METRIC model, which includes in its implementation radiometric calibration, computation of reflectance and biophysical variables, radiation balance, heat flux in the soil and parameterized iterative processes to obtain sensible heat. The balance of radiation, soil heat flux and real evapotranspiration estimated by the parameterized METRIC allowed us to obtain the influence of seasonality in the seasons of the year and the water conditions in the irrigated dwarf coconut crop. The parameterized METRIC was effective in estimating actual daily evapotranspiration in irrigated coconut palm crops during the dry season.

**keywords:** *cocos nucifera*, water demand, remote sensing, semiarid Brazil.

### 3 INTRODUCTION

The main coconut-producing region in Brazil is the Northeast, with production of 1,204,428 tons of fruit in 2020, which represented approximately 73.47% of national production (IBGE, 2020). In recent years, there has been a reduction in the availability of water for irrigation in several regions where coconut cultivation is an important economic activity, such as the coastal region of Ceará (Vale do Curu and Vale do Acaraú), the irrigated perimeter of São Gonçalo, Sousa-PB and Vale do São Francisco (MIRANDA *et al.*, 2019).

In this respect, it is necessary to improve the efficiency of water use in irrigated crops; therefore, the real daily evapotranspiration used as a basis for irrigation management determined through remote sensing techniques can be a quick and low-cost alternative in search of the use

water efficiency in coconut cultivation in the Brazilian semiarid region.

To this end, to apply the model using remote sensing techniques to estimate ETa, a trained user is needed who must calibrate (the identification of hot and cold pixels) in the METRIC model for each Landsat image, where the calibrations between users are independent and, therefore, not identical (MORTON *et al.*, 2013). Therefore, the appropriate selection of hot and cold pixels requires the skill of an expert and can be time-consuming and erroneous (SABOORI *et al.*, 2021). Generally, user intervention and selection are needed to select the locations in the image that represent these conditions and to assign ET estimates (ALLEN; TASUMI; TREZZA, 2007). However, the parameterized calibration method can allow for more complete tests of the uncertainty

and sensitivity of the METRIC model (MORTON *et al.*, 2013).

Therefore, this work proposed estimating the real evapotranspiration of the dwarf coconut tree crop using the parameterized METRIC algorithm through the energy balance in the northeastern semiarid region and comparing it with the standard Penman–Monteith method.

#### 4 MATERIALS AND METHODS

The study was carried out in an area located in the Municipality of Sousa, Paraíba, cultivated with dwarf coconut trees with the following coordinates: 6°49'57.77"S 38°18'16.67"W, at an altitude of 234 m above sea level. from the sea (Figure 1). The municipality's entire territorial area is located in the Rio do Peixe subbasin, belonging to the Piranhas-Açu River basin.

**Figure 1.** Location of the experimental area in the municipality of Sousa-PB, highlighting the sample plot with dwarf coconut tree cultivation (in yellow).



**Source:** Google Earth Pro, 2022.

According to the Koppen-Geiger classification, the climate in the municipality of Sousa is semiarid tropical (Bsh type), with an average temperature of 26.7 °C and an average annual rainfall of 872 mm, concentrated between January and April, with March being the month with the greatest precipitation. The predominant soils in the area are Red Argisol and Vertisol Haplic, and the natural vegetation is classified as hyperxerophilic Caatinga, leafless in the dry season, with an abundance of cacti and small plants (IBGE, 2023).

Initially, the images were chosen at the United States Geological Survey (USGS), taking into account the criteria of

days with low cloud cover to obtain better processing quality and meeting the research requirements and dates with the representation of land cover conditions in rainy, transition and dry periods; therefore, the three dates chosen were May 15th, June 16th and October 6th of 2016.

The images were generated by *Operational Land Imager - OLI* and *Thermal Infrared Sensor - TIRS* from the Landsat 8 satellite at approximately 09 hrs 45 min (local time), from orbit 216 and point 65 for the municipality of Sousa- PB. The images have a spatial resolution of 30 m and spectral resolution available in 16 bits, which means an intensity in each pixel

between 0 and 65,535 gray levels, ensuring greater detail in the information generated.

With the dates selected, the next step was to acquire climate data relating to

them from the National Institute of Meteorology-INMET at the automatic meteorological station located in São Gonçalo (INMET, 2016) (Table 1).

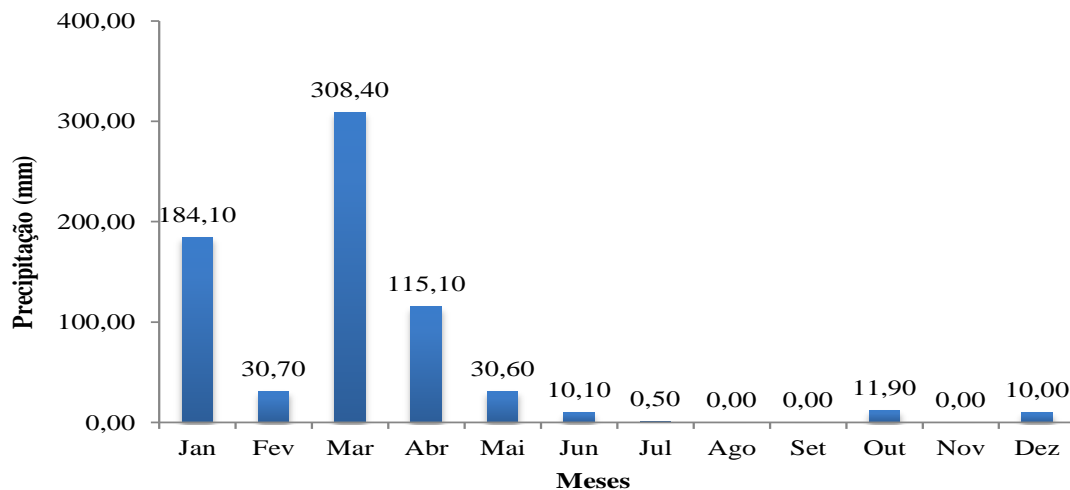
**Table 1.** Meteorological data used to obtain reference evapotranspiration ( $ET_{\theta}$ ) according to the Penman–Monteith method for the region of Sousa, PB.

Dates	Temp Max °C	Temp Min °C	Relative humidity (%)	Wind (m/s)	Sunstroke (hours)	Rad MJ/m <sup>2</sup> /day	ET $\theta$ (mm day <sup>-1</sup> )
05/15/2016	34.8	21.2	88	1.1	10.6	22.7	5.30
06/16/2016	34.0	20.0	81	2.5	10.5	21.5	5.36
10/06/2016	37.2	24.0	63	2.4	11.0	26.9	6.02

Source: INMET (2016)

Monthly precipitation data for 2016 for the region of Sousa, PB (Figure 2).

**Figure 2.** Monthly accumulated precipitation at the São Gonçalo-PB meteorological station in 2016.



Source: INMET (2016).

Based on data obtained from meteorological stations, the reference evapotranspiration ( $ET_{\theta}$ ) was determined for both days using Equation 1, which

$$ET_{\theta} = \frac{0,408 \cdot \Delta \cdot (R_n - G) + \gamma \cdot \left(\frac{900}{T_{ar} + 273}\right) \cdot U_2}{\Delta + \gamma \cdot (1 + 0,34 \cdot U_2)} \cdot (e_s - e_a) \quad (1)$$

Where  $ET_{\theta}$  is the reference evapotranspiration (mm.day<sup>-1</sup>);  $R_n$  is the radiation balance (MJ.m<sup>-2</sup> day<sup>-1</sup>);  $G$  is the

refers to a fundamental step to determine evapotranspiration using the METRIC algorithm.

heat flux in the soil (MJ.m<sup>-2</sup> day<sup>-1</sup>), considered to be of insignificant value when using daily calculations;  $T$  is the

average daily air temperature ( $^{\circ}\text{C}$ );  $U_2$  is the daily average wind speed at 2 m height ( $\text{ms}^{-1}$ );  $s_s$  is the vapor pressure at saturation (kPa);  $a$  is the current average daily vapor pressure (kPa);  $\Delta$  is the slope of the vapor pressure curve ( $\text{kPa}/^{\circ}\text{C}$ );  $\gamma$  is the psychrometric coefficient ( $\text{kPa}/^{\circ}\text{C}$ ) is considered constant,  $\gamma = 0.0622 \text{ kPa } ^{\circ}\text{C}^{-1}$ , as it is a function of atmospheric pressure, which varies very little throughout the year (95.03 kPa), and the latent heat of water evaporation, which is little affected by temperature, with an average value equal to  $2.45 \text{ MJ kg}^{-1}$  being recommended.

The FAO-PM 56 method also allows calculating the actual crop evapotranspiration ( $ET_c$ ) by multiplying ( $ET_{\theta}$ ), determined by the Penman-Monteith method, by the Crop Coefficient ( $K_c$ ), according to recommendations by Allen *et al.* (1998) Equation 2.

$$ET_c = ET_{\theta} \cdot K_c \quad (2)$$

For the dwarf coconut tree in the stadium intermediate growth stage, after the fifth year in the Brazilian semiarid region, an average crop coefficient  $K_c$  of 1.00 was

$$R_n = R_{s,inc} \cdot (1 - \alpha_s) - R_{ol,emi} + R_{ol,atm} - (1 - \varepsilon_0) \cdot R_{ol,atm} \quad (4)$$

Where  $R_{s,inc}$  is the incident shortwave radiation;  $R_{ol,emi}$  is the longwave radiation emitted by each pixel;  $R_{ol,atm}$  is the longwave radiation emitted by the atmosphere in the direction of each pixel (ALLEN *et al.*, 2002);  $\alpha_s$  is the surface albedo of each pixel; and  $\varepsilon_0$  is the emissivity of each pixel (ALLEN *et al.*, 2007).

In determining the daily radiation balance at the surface ( $R_{n24h}$ ,  $\text{W m}^{-2}$ ), using a model calibrated for conditions

used, a value recommended by Allen *et al.* (1998) and used by Miranda *et al.* (2007).

ETa was estimated from the latent heat flux density, obtained as a residue of the energy balance (Equation 3), by the parameterized METRIC model, which includes in its implementation radiometric calibration, calculation of reflectance and biophysical variables, radiation balance, heat flow in the soil and parameterized iterative processes to obtain sensible heat.

$$LE = R_n - G - H \quad (3)$$

Where  $LE$  = Latent heat flux ( $\text{W}/\text{m}^2$ );  $R_n$  = net radiation at the surface ( $\text{W}/\text{m}^2$ );  $G$  = Soil heat flux ( $\text{W}/\text{m}^2$ ) and  $H$  = Sensible heat flux ( $\text{W}/\text{m}^2$ ).

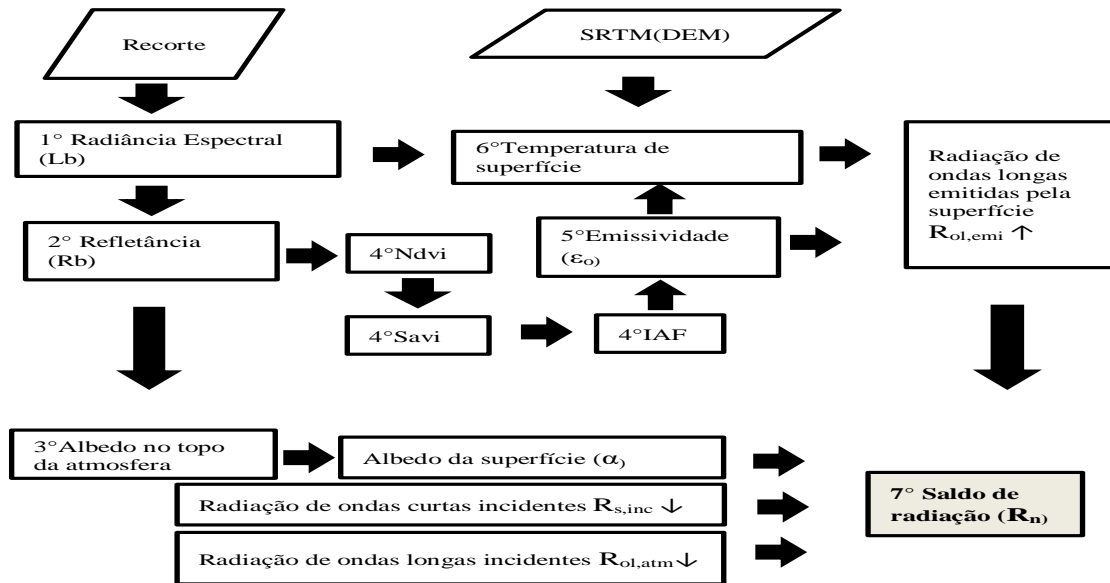
The radiation balance of a surface represents the amount of energy in the form of electromagnetic waves available to be distributed among the energy flows necessary for the processes of evapotranspiration, air heating, soil heating and photosynthesis. Calculated from equation 4 (SABOORI *et al.*, 2021).

observed in the Brazilian semiarid region, Equation 5 was used.

$$R_{n24h} = R_{s24h} (1 - \alpha_s) - 123 \cdot \tau_{sw24} \quad (5)$$

Where  $R_{s24h}$  is the daily global solar radiation ( $\text{W m}^{-2}$ );  $\alpha_s$  is the surface albedo; and  $\tau_{sw24}$  is the daily average transmissivity used to convert the daily balance into  $\text{MJ m}^{-2}$ . The factor 0.0864 is multiplied by  $R_{n24h}$ , as already used in several applications by several researchers.

**Figure 3.** Diagram of computational processing steps to obtain the surface radiation balance (Rn) using the mapping evapotranspiration algorithm at high resolution with internalized calibration (METRIC).



Source: Authors' organization (2023)

The heat flow in the soil is the rate of heat stored by the soil and vegetation and was obtained through Equation 6,

$$G = \left[ \frac{T_s}{\alpha_s} \cdot (0,0038 \cdot \alpha_s + 0,0074 \cdot \alpha_s^2) \cdot (1 - 0,98 \cdot NDVI^4) \right] \cdot R_n \tag{6}$$

Where  $T_s$  is the surface temperature and  $\alpha_s$  is the surface albedo (ALLEN *et al.*, 2002). For the purpose of correcting soil heat flux values for bodies of water, where  $NDVI < 0$ , the following expression can be used:  $G = 0.5 \cdot R_n$ , according to Allen *et al.* (2002).

The sensible heat flux H at each pixel was estimated based on wind speed and ground temperature using an internal calibration of the near-surface temperature difference dT between two surface levels (ALLEN *et al.*, 2013):

$$H = \rho c_p \frac{(a+bT_s)}{r_{ah}} \tag{7}$$

Where  $\rho$  is the specific mass of the air,  $c_p$  is the specific heat of the air, a and b are calibration constants for the temperature

developed by Bastiaanssen (2000), which represents the values close to the satellite passage.

difference between two levels  $Z_1$  and  $Z_2$ ,  $T_s$  is the surface temperature (°C) and  $r_{ah}$  is the aerodynamic resistance to heat transport ( $sm^{-1}$ ). The soil surface temperature is provided by the satellite.

The air temperature difference close to the ground surface, dT, was calculated assuming that this difference can be obtained as a function of the radiometric temperature of each pixel, according to Equation 8:

$$dT = a + b \cdot T_{ar} \tag{8}$$

Where a and b are coefficients obtained based on the conditions observed in the anchor pixels (hot and cold) and  $T_{ar}$  is the temperature of each pixel (°C). The coefficients a and b are determined using

two pairs of values for  $dT$  and  $T_s$  by Equations 9 and 10:

$$a = \frac{dT_q - dT_f}{T_{S_q} - T_{S_f}} \quad (9)$$

$$b = \frac{dT_q - a}{T_{S_q}} \quad (10)$$

Where  $T_{S_q}$  and  $T_{S_f}$  are the surface temperatures at the hot and cold pixels fitted to the elevation data for each pixel in the image using the digital elevation model.

The temperature differences in the hot pixels  $dT_q$  are obtained by equation 11.

$$dT_q = \frac{H_q \cdot r_{ahq}}{\rho_q \cdot C_p} \quad (11)$$

In the hot pixels, H is calculated by equation 12.

$$H_q = R_{nq} - Gq - 0,10 \cdot \lambda \cdot ET_0 \quad (12)$$

Where  $\rho$  ( $\text{kg m}^{-3}$ ) is the specific mass of the air,  $c_p$  is the specific heat of the air at constant pressure ( $\text{J kg}^{-1} \text{K}^{-1}$ ) and  $T_{sup}$  ( $^{\circ}\text{C}$ ), and  $R_n$  ( $\text{W m}^{-2}$ ) and  $G$  ( $\text{W m}^{-2}$ ) were obtained exactly at the coordinates of the hot pixels in the image.

The temperature differences in the cold  $dT_f$  pixels are obtained by equation 13.

$$dT_f = \frac{H_f \cdot r_{ahf}}{\rho_f \cdot C_p} \quad (13)$$

Where  $r_{ahf}$  is estimated for the stability conditions and the surface roughness of the cold pixel;  $\rho_f$  is the air density calculated for the cold pixel; and  $C_p$  is the specific heat of the air at constant pressure ( $\text{J kg}^{-1} \text{K}^{-1}$ ).

$$\lambda = [2,501 - 0,00236(T_s - 273,15)] \cdot 10^6 \quad (16)$$

The reference evapotranspiration fraction ( $ET_r F$ ) is calculated as the ratio of the calculated instantaneous ET ( $ET_{inst}$ ) of

The value of H in the cold pixel is calculated by equation 54.

$$H_f = R_{nf} - Gf - 1,05 \cdot \lambda \cdot ET_0 \quad (14)$$

In this step, the algorithm selects the hot pixel and cold pixel candidates, which are combined in pairs and applied to the function that obtains the coefficients a and b for application in Equation 8, which determines the temperature gradient  $dT$  and is used in the calculation of H (Equation 7).

In the selection stage of anchor pixels (cold and hot), they followed the methodology of Allen *et al.* (2013). The cold pixel was selected from the 20% coldest and most vegetated points in the images, selecting the 5% of the coldest and most vegetated areas in the images, which comprises 1% of the coldest pixels in the irrigated area. It has an ETrF value of 1.05 when fully vegetated. The hot pixel was selected from the 2% of the hottest and least vegetated area of the image, identifying the hottest 20% of the 10% of lowest vegetated values and still having a  $hot$  ETrF Reference Evapotranspiration Fraction (crop coefficient) associated with the ETrF of a bare soil ETrF<sub>bare</sub>.

Evapotranspiration- ET at the time of the satellite image is calculated for each pixel by dividing LE by the latent heat of vaporization, giving rise to Equation 15:

$$ET_{ins} = 3,600 \cdot \frac{LE}{\lambda \rho_w} \quad (15)$$

Where  $ET_{inst}$  = daily evapotranspiration ( $\text{mm h}^{-1}$ ); 3,600 seconds to hours conversion,  $\rho_w$  is the density of water ( $1000 \text{ kgm}^{-3}$ ) and  $\lambda$  is the latent heat of vaporization ( $\text{J kg}^{-1}$ ), which is calculated using Equation 16:

each pixel to the reference evapotranspiration ( $ET_r$ ) calculated from meteorological data applied to Equation 17,

according to Allen *et al.* (2007), who assume that  $ET_r F$  remains constant throughout the day.

$$ET_r F = \frac{ET_{inst}}{ET_r} \quad (17)$$

Where  $ET_{inst}$  is from Equation 15 ( $\text{mm h}^{-1}$ ) and  $ET_r$  is the hourly reference evapotranspiration according to FAO-56 (ALLEN *et al.*, 1998). In the calculation of  $ET_r F$  in the above, each pixel refers to a single value for  $ET_{inst}$ , which is derived from a common value for  $ET_r$  derived from representative weather station data.

Finally, the  $ET_{r24h}$  ( $\text{mm day}^{-1}$ ) is calculated by Equation 61 for each pixel of the image:

$$ET_{r24h} = C_{rad} (ET_r F) (ET_{r,24}) \quad (18)$$

Since  $ET_r F$  is assumed equal to the  $ET_r F$  determined at the time of satellite passage;  $ET_{r,24}$  = the daily reference evapotranspiration; and  $C_{rad}$  = correction term used in sloped terrain for variation in 24 hours versus instantaneous energy availability (ALLEN *et al.*, 2007).

#### 4.1 Validation of results: error analysis between 24 h ET - Parameterized METRIC and Penman–Monteith Method

In analyzing the precision of evapotranspiration estimates obtained by METRIC and Penman–Monteith, the mean absolute error (EAM) and the mean relative error (ERM) obtained through Equations 19 and 20 described below were used:

$$EAM = \frac{1}{N} \sum_{i=1}^N |ET_{Metric} - ET_{Penman}| \quad (19)$$

$$RM = \frac{100}{N} \sum_{i=1}^N \left| \frac{ET_{Metric} - ET_{Penman}}{ET_{Penman}} \right| \quad (20)$$

Where  $ET_{Metric}$  and  $ET_{Penman}$  correspond to the evapotranspiration values using the parameterized METRIC and the Penman–Monteith method, respectively.

## 5 RESULTS AND DISCUSSION

### 5.1 Penman–Monteith method

Table 2 presents the values of real evapotranspiration ( $ET_{rFAO}$ ,  $\text{mm day}^{-1}$ ), inferred using the Penman–Monteith method, estimated by multiplying  $ET_{\theta}$  by the coconut crop coefficient ( $K_c$ ) for May 15th, June 16th and October 6th of 2016.

**Table 2.** Real evapotranspiration data using the FAO-56 standard physical model (PENMAN-MONTEITH) for Sousa, PB.

Image dates	ET $\theta$ Reference ( $\text{mm day}^{-1}$ )	ET $r$ ( $K_c=1.00$ ) ( $\text{mm day}^{-1}$ )
05/15/2016	5.30	5.30
06/16/2016	5.36	5.36
10/06/2016	7.41	7.41

\* $ET_{rFAO} = ET_{\theta}$  (Penman) \* Cultivation Coefficient  $K_c$

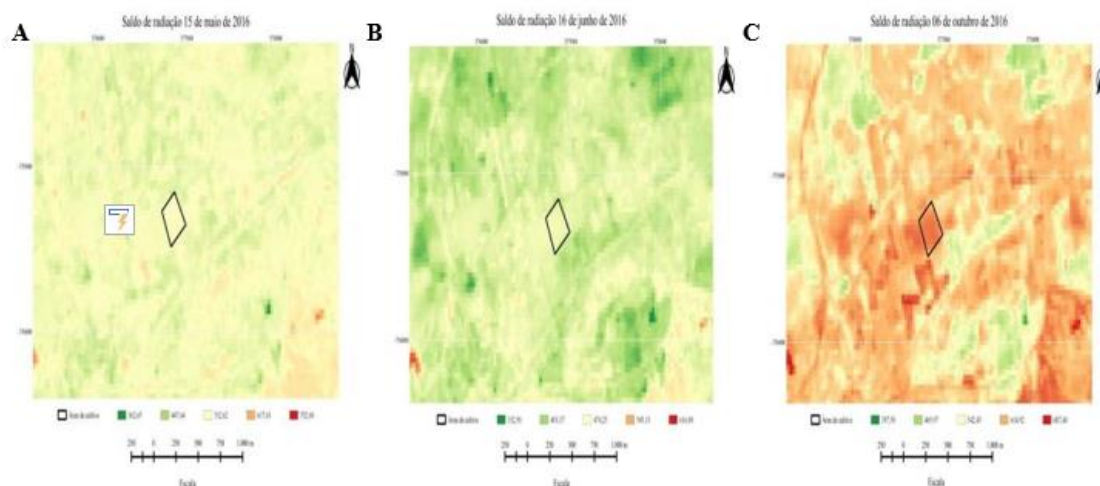
Source: Authors' organization (2023)

## 5.2 Radiation balance (Rn)

In Figure 4, the thematic maps of the instantaneous radiation balance at the surface are presented for the dates May

15th (A), June 16th (B) and October 6th (C) of 2016. In the irrigated area in the coconut orchard-dwarf, the values were between 490.13 and 687.40 W m<sup>-2</sup>.

**Figure 4.** Thematic chart of the surface radiation balance (Rn) - METRIC (*Mapping Evapotranspiration at High Resolution with Internalized Calibration*) for the municipality of Sousa, PB on May 15th (A), June 16th (B) and October 6th (C) in 2016.



**Source:** Authors' organization (2023)

On May 15th (rainy season), the radiation balance presented a value close to 532.62 W m<sup>-2</sup>, while June 16th was between 403.37 and 474.25 W m<sup>-2</sup>, that is, less energy is available to be distributed in the process of soil heating, air heating and evapotranspiration.

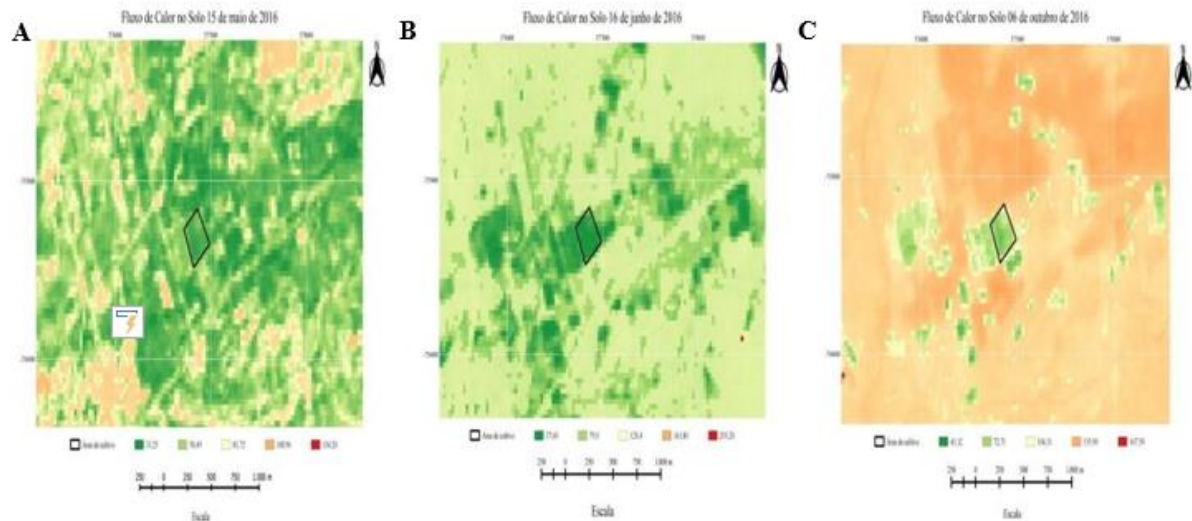
In the period of greatest drought, October 6th, a range of 614.92 to 687.4 W m<sup>-2</sup>, the highest radiation balance found within the area, in the same way it was observed in the cultivation of dwarf bananas in the dry period in the southern region of Ceará in the study by Diniz *et al.* (2021) with the metric model. This difference in the radiation balance can be influenced by seasonality depending on the

time of year, water regime and vegetation cover (SANTOS *et al.*, 2021; CARVALHO; MOURA; SILVA, 2018).

## 5.3 Soil heat flow (G)

The magnitudes of heat flux in the soil for the municipality of Sousa can be observed in the thematic maps in Figure 5. For the dates analyzed, the heat flux values in the soil within the area were between 33.25 and 72.71 W m<sup>-2</sup>, with a lower value in the rainy season and a higher value in the dry season. These results are similar to those found by Diniz *et al.* (2021) in the dwarf banana crop and Carvalho, Moura and Silva (2018) in the sugarcane crop.

**Figure 5.** Thematic chart of heat flow in surface soil (G) - METRIC (Mapping Evapotranspiration at High Resolution with Internalized Calibration) for the municipality of Sousa, PB on May 15th (A), June 16th (B) and October 6th (C) in 2016.



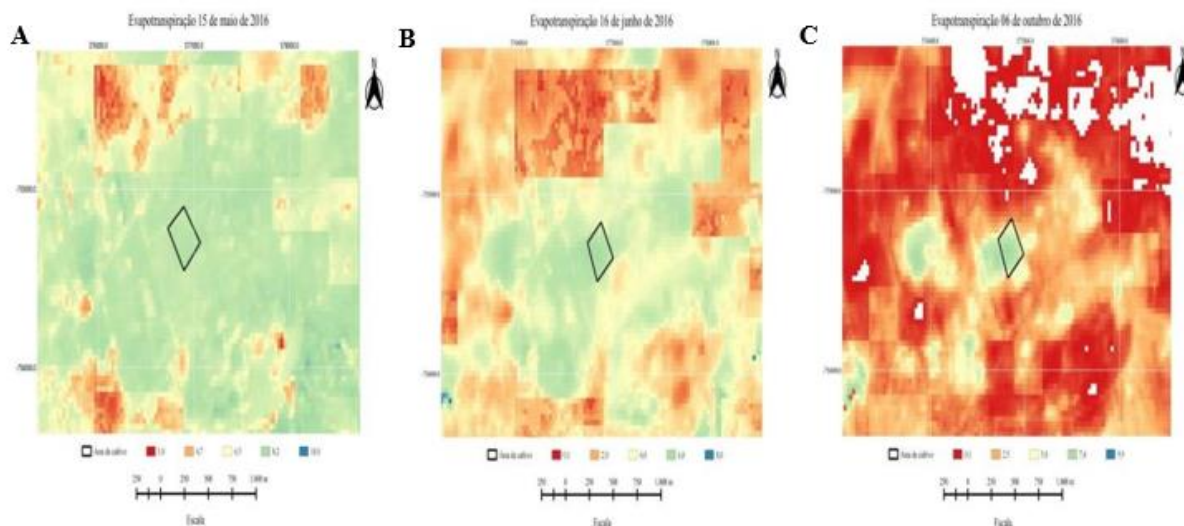
Source: Authors' organization (2023)

#### 5.4 Real daily evapotranspiration (E<sub>Tr</sub> 24 h)

The real daily evapotranspiration in the coconut grove for the municipality of

Sousa on the dates studied was 8.2 mm day<sup>-1</sup> for the 15th of May (A), on the 16th of June 6.0 mm day<sup>-1</sup> (B) and for October 6th 7.4 mm day<sup>-1</sup> (C) (Figure 6).

**Figure 6.** Thematic chart of real daily evapotranspiration (ETr 24 h) - METRIC (Mapping Evapotranspiration at High Resolution with Internalized Calibration) for the municipality of Sousa, PB on May 15th (A), June 16th (B) and October 6th (C) in 2016.



**Source:** Authors' organization (2023)

The current daily evapotranspiration estimated by the METRIC algorithm parameterized in the image of May 15th ( $8.2 \text{ mm day}^{-1}$ ) may have been underestimated, motivated by the fact that on May 14th (the day before image collection), there was significant rainfall in the area of 21.6 mm immediately before the satellite's passage (between 6 and 7 am). This is a limitation for the application of the parameterized METRIC, since high evaporation values for the hot pixel decrease the hydrological contrast between

the anchor pixels and may have led to errors in the ETa estimates.

On the dates of June and October, they observed the seasonal effect of Rn, water conditions and vegetation, with evapotranspiration occurring at  $6.0 \text{ mm d}^{-1}$  and  $7.4 \text{ mm d}^{-1}$ , respectively.

### 5.5 Validation between evapotranspiration obtained with the parameterized METRIC algorithm and the Penman–Monteith method

**Table 5.** Comparison between the real daily evapotranspiration (ETc) obtained by the FAO-56 standard physical model (Penman - Monteith) and the real average daily evapotranspiration (ETa) obtained by the Mapping Evapotranspiration algorithm at High Resolution with Internalized Calibration (METRIC) parameterized for a coconut palm area located in Sousa-PB.

Dates	ETa (Metric)	ETc (Penman)	Relative Error (%)	Absolute error ( $\text{mm day}^{-1}$ )
05/15/2016	8.2	5.30	54.71	2.90
06/16/2016	6.0	5.36	11.94	0.64
10/06/2016	7.4	7.41	0.13	0.01

**Source:** Authors' organization (2023)

Through Table 5, it was observed that the greatest divergence found in the real daily evapotranspiration obtained by the parameterized METRIC and the Penman–Monteith method was on the 15th of May, as previously explained, probably because on the 14th of May, there was precipitation (21.6 mm). Therefore, the model was developed to be applied in semiarid regions in irrigated areas during the dry season.

In June, a relative error in the acceptable limit was observed, as reported in the literature for ETa estimates from remote sensing data (GLENN *et al.*, 2007). Errors found equal to or less than 12.0% are considered a satisfactory and acceptable level of precision.

The greatest precision was found in the month of October, within the region's driest period, presenting the lowest results for ERM (0.13%) and EAM (0.01). For this reason, it can be said that application of the parameterized model in periods further away from the influences of the rainy season has a better estimate of real evapotranspiration in irrigated areas. Similar results were found by Medeiros *et al.* (2021) in the SEBAL model, presenting the lowest values in the dry periods of ERM and EAM of 3% and 0.08mm day<sup>-1</sup>, respectively.

## 6 CONCLUSION

The radiation balance, heat flux in the soil and real evapotranspiration estimated by the parameterized METRIC allowed us to obtain the influence of seasonality in the times of the year and the water conditions in the irrigated dwarf coconut tree crop.

The parameterized METRIC was effective in estimating real daily evapotranspiration in irrigated coconut crops during the dry season. The parameterization of anchor pixel selection

allows a drastic reduction in model processing time, with the possibility of testing many pairs of anchor pixels in the calibration process. This is an important result of this research since the processing time and availability of ETa maps are essential issues in operational monitoring for irrigated agriculture.

## 7 ACKNOWLEDGMENT

The Postgraduate Course in Agricultural Engineering (PPGEA) and the Coordination for the Improvement of Higher Education Personnel (CAPES).

## 8 REFERENCES

- ALLEN, RG; BURNETT, B.; KRAMBER, W.; HUNTINGTON, J.; KJAERGAARD, J.; KILIC, A.; KELLY, C.; TREZZA, R. Automated calibration of the metric-landsat evapotranspiration process. **Journal of the American Water Resources Association**, Herndon, vol. 49, n. 3, p. 563-576, 2013.
- ALLEN, RG; PEREIRA, LS; RAES, D.; SMITH, M. **Crop evapotranspiration: Guidelines for computing crop water requirements**. Rome: FAO, 1998. (Irrigation and Drainage Paper n. 56).
- ALLEN, RG; TASUMI, M.; TREZZA, R. Satellite-Based energy balance for mapping evapotranspiration with internalized calibration (METRIC) – Model. **Journal of Irrigation and Drainage Engineering**, New York, vol. 133, no. 4, p. 380-394, 2007.

- ALLEN, RG; TASUMI, M.; TREZZA, R.; WATERS, R.; BASTIAANSEN, W. **SEBAL** - Surface Energy Balance Algorithm for Land. Advanced training and Users Manual. Version 1.0. Kimberly: University of Idaho, 2002.
- BASTIAANSEN, WGM SEBAL – Based Sensible and Latent Heat Fluxes in the Irrigated Gediz Basin, Turkey. **Journal of Hydrology**, Amsterdam, v. 229, no. 1, p. 87-100, 2000.
- CARVALHO, HFDS; MOURA, MSBD; SILVA, TGFD Radiation and energy fluxes in preserved caatinga and sugarcane in the semiarid region. **Brazilian Meteorology Magazine**, São José dos Campos, v. 33, no. 3, p. 452-458, 2018.
- DINIZ, RRS; CORDÃO, MA; WAR, HOC; OLIVEIRA, CW Real evapotranspiration of dwarf banana determined by the METRIC algorithm in the semiarid region of Ceará. **Irriga**, Botucatu, v. 26, no. 3, p. 701-716, 2021.
- GLENN, EP; HUETE, AR; NAGLER, PL; HIRSCHBOECK, KK; BROWN, P. Integrating remote sensing and ground methods to estimate evapotranspiration. **Critical Reviews in Plant Sciences**, Las Vegas, vol. 26, no. 3, p. 139-168, 2007.
- IBGE. Environmental Information Database - BDIA. Rio de Janeiro: IBGE, 2022. Available at: <https://bdiaweb.ibge.gov.br/#/consulta/pedologia>. Accessed on: 15. Jan. 2023.
- IBGE. CIDER. **Municipal Agricultural Production**. Table 5457 – Area planted or intended for harvesting, harvested area, quantity produced, average yield and production value of temporary and permanent crops. Rio de Janeiro: IBGE, 2020. Available at: <https://sidra.ibge.gov.br/tabela/5457>. Accessed on: 08 Apr. 2022.
- INMET. **Annual historical data**. Brasília, DF: INMET, 2016. Available at: <https://bdmep.inmet.gov.br/>. Accessed on: 18 September. 2020.
- MEDEIROS, JLS; JESUS, IS; SILVA, TJRD; NASCIMENTO, MB; CEZÁRIO, JA; DE PAIVA, W.; SANTOS, LL; CAMPOS, GM; MOITINHO, EB; FONSECA, LLS Estimation of real evapotranspiration using geotechnology in the semiarid region, Bahia, Brazil. **Ibero-American Journal of Environmental Sciences**, Aracaju, v. 12, no. 6, p. 360-376, 2021.
- MIRANDA, FR; ROCK, ABS; GUIMARÃES, VB; SILVA, ES; LIMA, GCM; SANTOS, MMS Efficiency of water use in irrigation of dwarf coconut trees. **Irriga**, Botucatu, v. 24, no. 1, p. 109-124, 2019.
- MIRANDA, FR; GOMES, ARM; OLIVEIRA, CHC; MONTENEGRO, AAT; BEZERRA, FML Evapotranspiration and cultivation coefficients of dwarf green coconut trees in the coastal region of Ceará. **Agricultural Science Magazine**, Fortaleza, v. 38, no. 2, p. 129-135, 2007.
- MORTON, C. G.; HUNTINGTON, JL; POHLL, GM; ALLEN, RG; MCGWIRE, K.C.; BASSETT, SD Assessing calibration uncertainty and automation for estimating evapotranspiration from agricultural areas using METRIC. **Journal of the American Water Resources Association**, Herndon, v. 49, n. 3, p. 549-562, 2013.

SANTOS, JM; LOPES, PMO; MOURA, GBD; SILVA, AS; SILVA, LBJ; OLIVEIRA JÚNIOR, JG Analysis of irrigated sugarcane fields with biophysical parameters by remote sensing in northeastern Brazil. **Irriga**, Botucatu, v. 26, no. 3, p. 638-663, 2021.

SABOORI, M.; MOKHTARI, A.; AFRASIABIAN, Y.; DACCACHE, A.; ALAGHMAND, S.; MOUSIVAND, Y. Automatically selecting hot and cold pixels for satellite actual evapotranspiration estimation under different topographic and climatic conditions. **Agricultural Water Management**, Amsterdam, v. 248, no. 1, p. 106763, 2021.